

**Supporting Information**

**Dipole Fluctuation and Structural Phase Transition in  
Hydrogen-Bonding Molecular Assemblies of  
Mononuclear Cu<sup>II</sup> Complexes with Polar Fluorobenzoate  
Ligands**

*Kiyonori Takahashi \* Yuji Miyazaki, Shin-ichiro Noro, Motohiro Nakano,  
Takayoshi Nakamura, Tomoyuki Akutagawa\**

\*E-mail: ktakahashi@es.hokudai.ac.jp

**Table of Contents**

<b>Experimental Section</b>	<b>S2</b>
<b>Differential Scanning Calorimetry</b>	<b>S3</b>
<b>X-ray Oscillation Photograph</b>	<b>S3</b>
<b>Crystallographically Independent Molecules in the Crystals.</b>	<b>S4–S6</b>
<b>Summary of Hydrogen Bonding Distance</b>	<b>S7</b>
<b>Temperature- and Frequency-Dependent Dielectric Constant for crystals 1 and 2</b>	<b>S8</b>
<b>Potential Energy Curves for F<sub>x</sub>BA Ligand Rotation</b>	<b>S9–S10</b>

## Experimental Section

**DFT calculations.** Potential energy curves for the molecular rotations of 4-FBA, 3-FBA, and 3,4-F<sub>2</sub>BA ligands were obtained by a theoretical DFT calculation based on a B3LYP/3-21G(*d*) basis set. Atomic coordinates for the calculations were obtained from each crystal structures **1** at 300 K, **2** at 250 K, and **3** at 300 K. One fluorobenzoate (F<sub>x</sub>BA) molecule surrounding by neighboring four F<sub>x</sub>BA ligands was rotated every 30 ° along the C–COO<sup>−</sup> axis, and a single point energy for every rotation was obtained. The potential energy at a rotation angle  $\phi = 0^\circ$  was defined as  $\Delta E = 0 \text{ kJ mol}^{-1}$ , and the  $\phi - \Delta E$  plots were determined for crystals **1**, **2**, and **3**.

## Differential Scanning Calorimetry

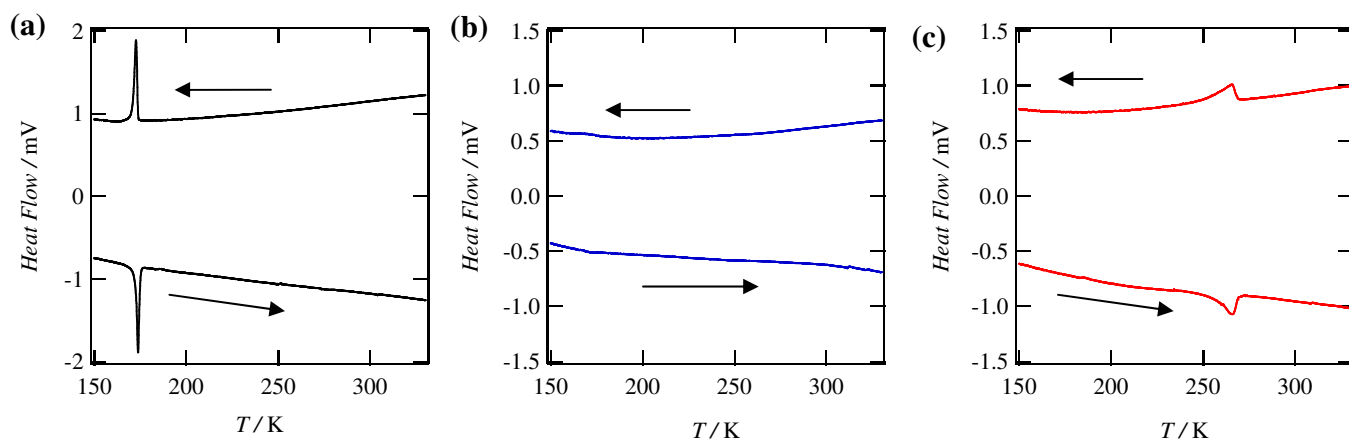


**Figure S1.** DSC charts of crystals of (a) **1**, (b) **2**, and (c) **3** at the temperature range from 150 to 320 K.

## X-ray Oscillation Photograph

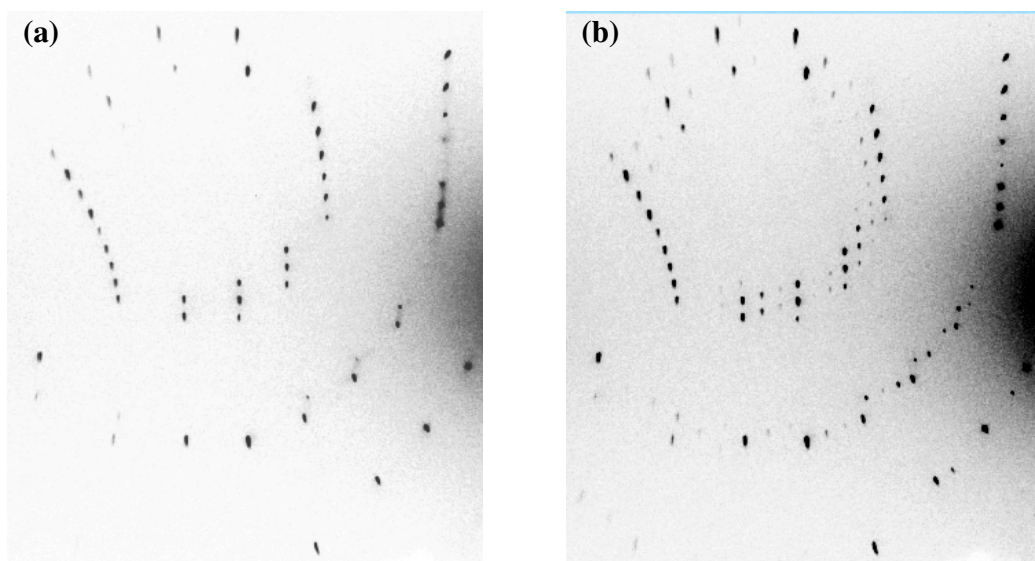


**Figure S2.** Changes in diffraction spots for crystal **2** with temperature changes. X-ray oscillation photograph of the same sample measured under the same conditions except for the temperature at (a) 180 and (b) 170 K.

### Crystallographically Independent Molecules in the Crystals.

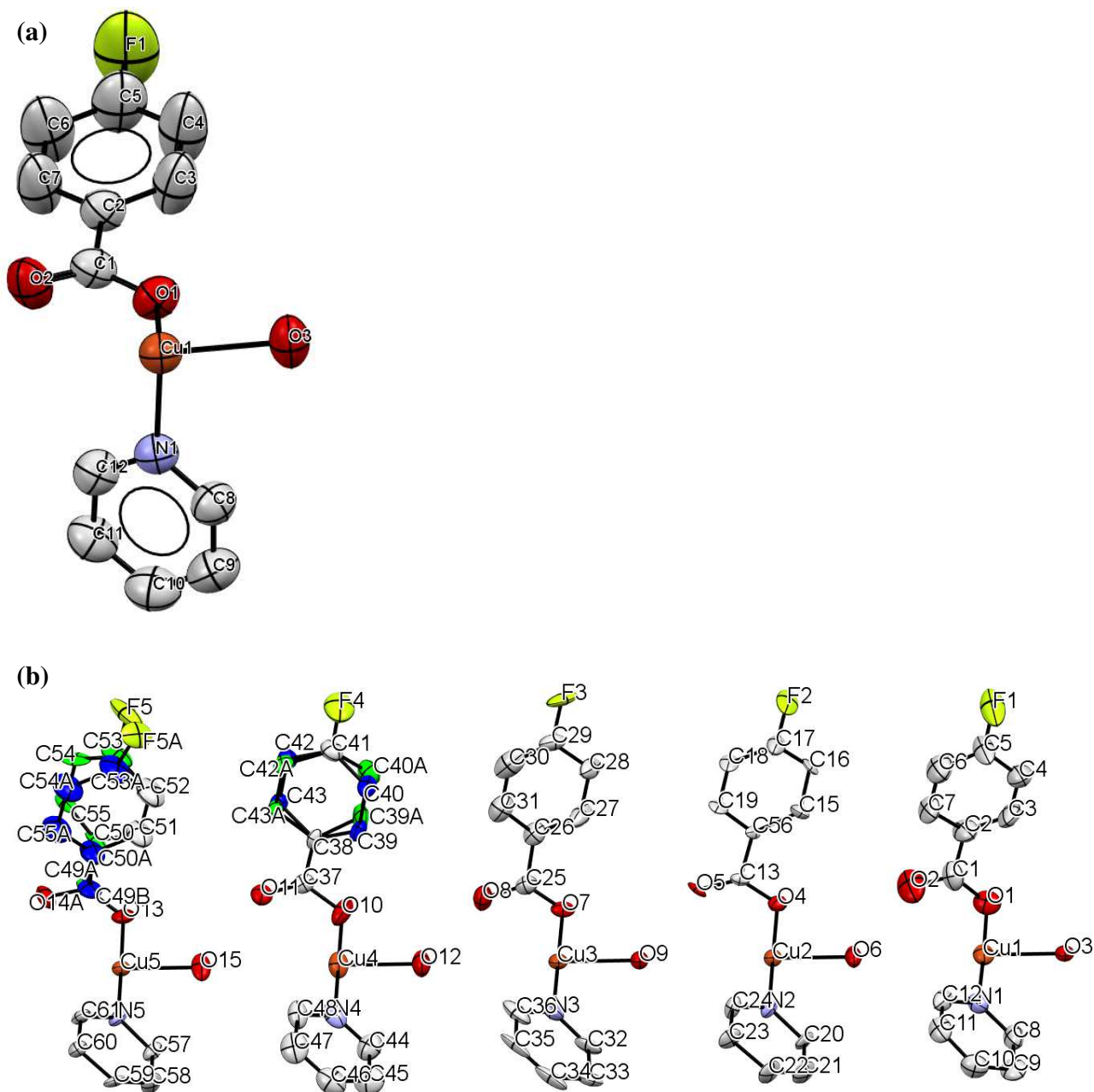


**Figure S3.** Crystallographically independent molecular structures and atomic numbers of the crystal **1** for (a) the high and (b) low temperature phases, respectively. Gray, red, purple, blown, and yellow atoms correspond to carbon, oxygen, copper, fluorine, respectively. Hydrogen atoms are omitted for the clarity.

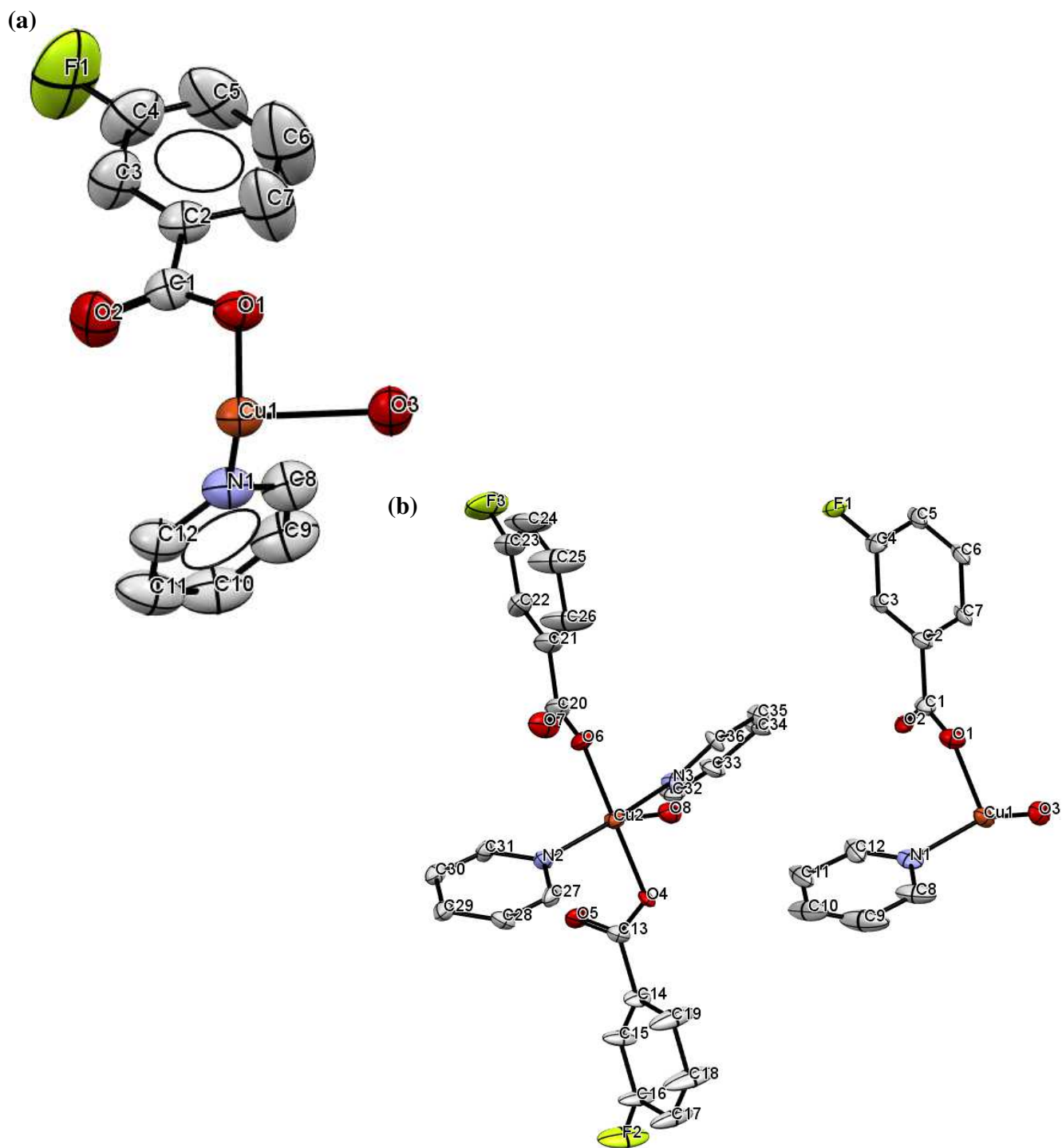


**Figure S4.** Crystallographically independent molecular structures and atomic numbers of the crystal **2** for (a) the high and (b) low temperature phases, respectively. Gray, red, purple, blown, and yellow atoms correspond to carbon, oxygen, copper, fluorine, respectively. Hydrogen atoms are omitted for the clarity.

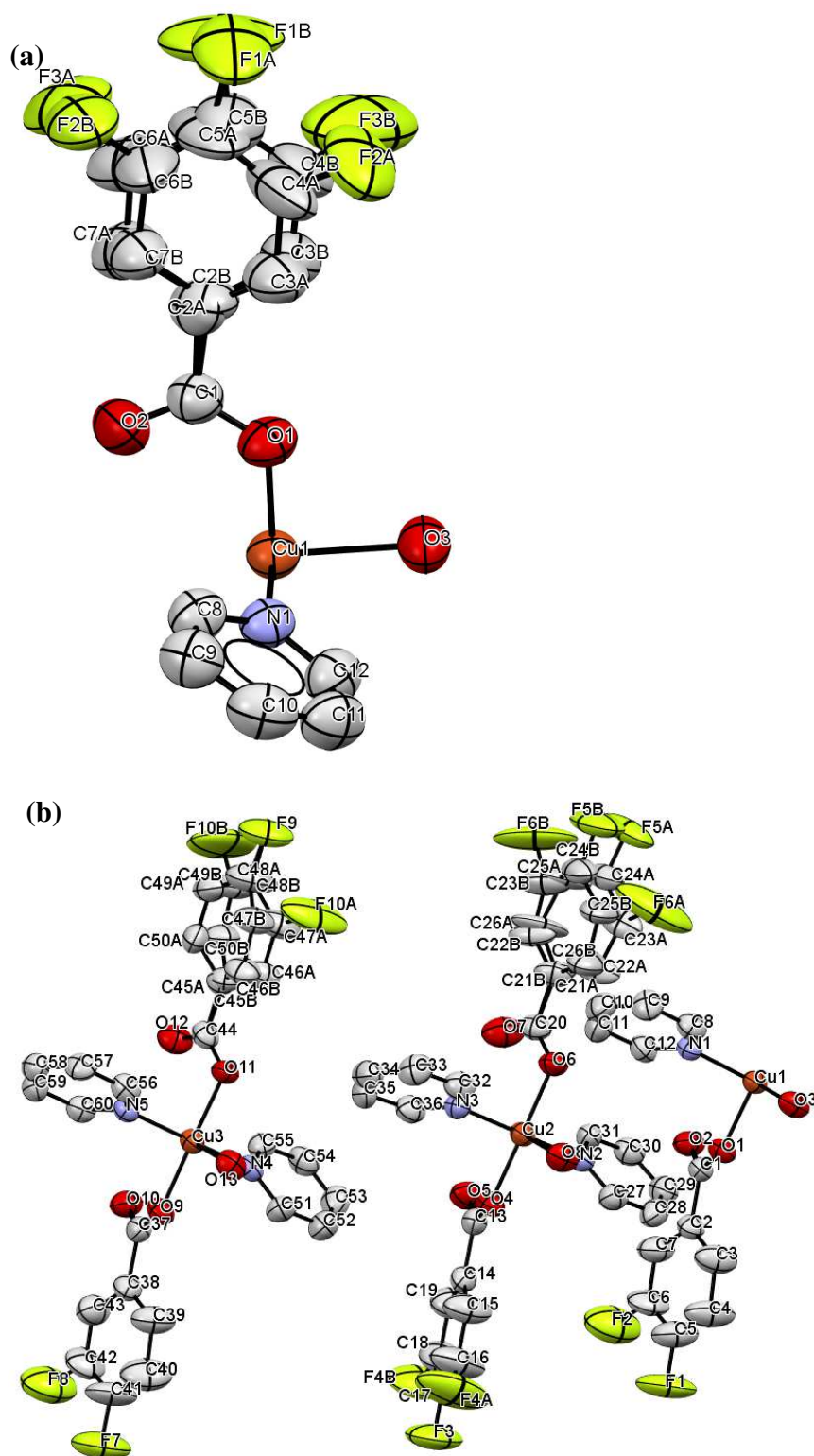


**Figure S5.** Crystallographically independent molecular structures and atomic numbers of the crystal **3** for (a) the high and (b) low temperature phases, respectively. Gray, red, purple, blown, and yellow atoms correspond to carbon, oxygen, copper, fluorine, respectively. Hydrogen atoms are omitted for the clarity.



**Table S1** Hydrogen bonding distance between oxygen atom in H<sub>2</sub>O ligand and free oxygen in F<sub>x</sub>BA.

Crystal	Oxygen in H <sub>2</sub> O	Free oxygen in F <sub>x</sub> BA	$d_{O-O} / \text{\AA}$	Percentage difference (%)
<b>1</b> in HTP (300 K)	O3	O2	2.772	0
<b>1</b> in LTP (170 K)	O2	O6	2.707	-2.34
	O5	O9	2.83	2.09
	O8	O12	2.751	-0.76
	O11	O15	2.761	-0.40
	O14A	O3	2.779	0.25
<b>2</b> in HTP (300 K)	O3	O2	2.808	0
<b>2</b> in LTP (100 K)	O5	O2	2.746	-2.21
	O5	O4	2.875	2.39
	O10	O7	2.88	2.56
	O10	O9	2.743	-2.31
	O15	O12	2.724	-2.99
	O15	O14	2.736	-2.56
<b>3</b> in HTP (300 K)	O3	O2	2.76	0
<b>3</b> in LTP (240 K)	O3	O2	2.796	1.30
	O8	O5	2.733	-0.978
	O8	O7	2.712	-1.74
	O13	O10	2.815	1.99
	O13	O12	2.761	0.03



### Temperature- and Frequency-Dependent Dielectric Constant for crystals 1 and 2

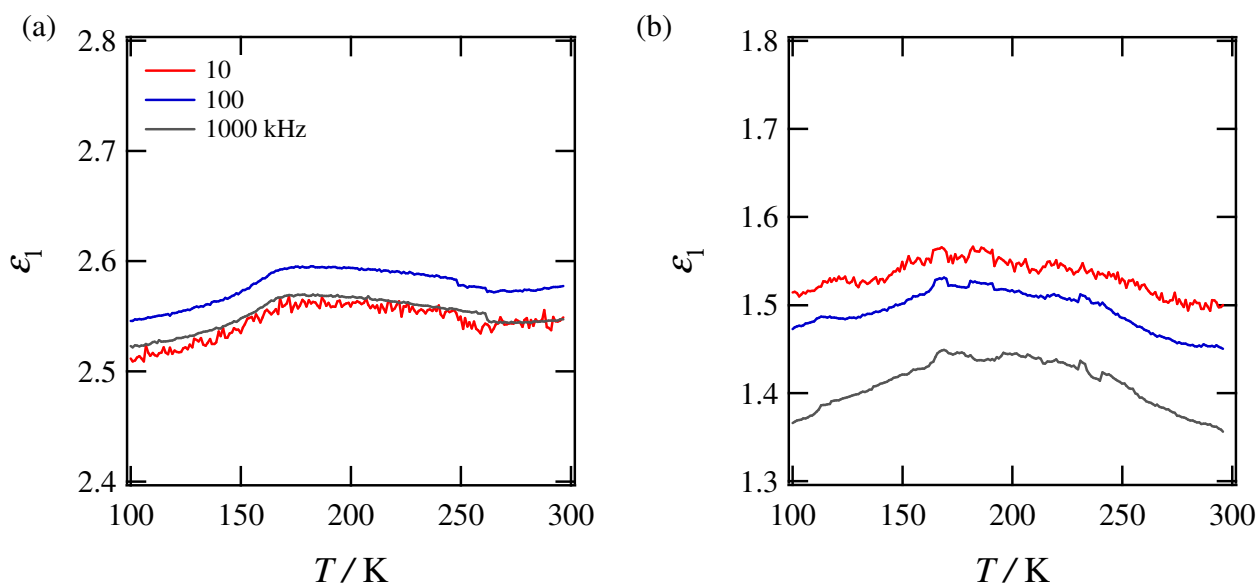


**Figure S6.** Temperature- and frequency dependent real part of dielectric constant for crystals of (a) **1** and (b) **2**, respectively. Red, blue and grey lines correspond to the plot for the frequencies of 10, 100 and 1000 kHz, respectively.

## Potential Energy Curves for F<sub>x</sub>BA Ligand Rotation.

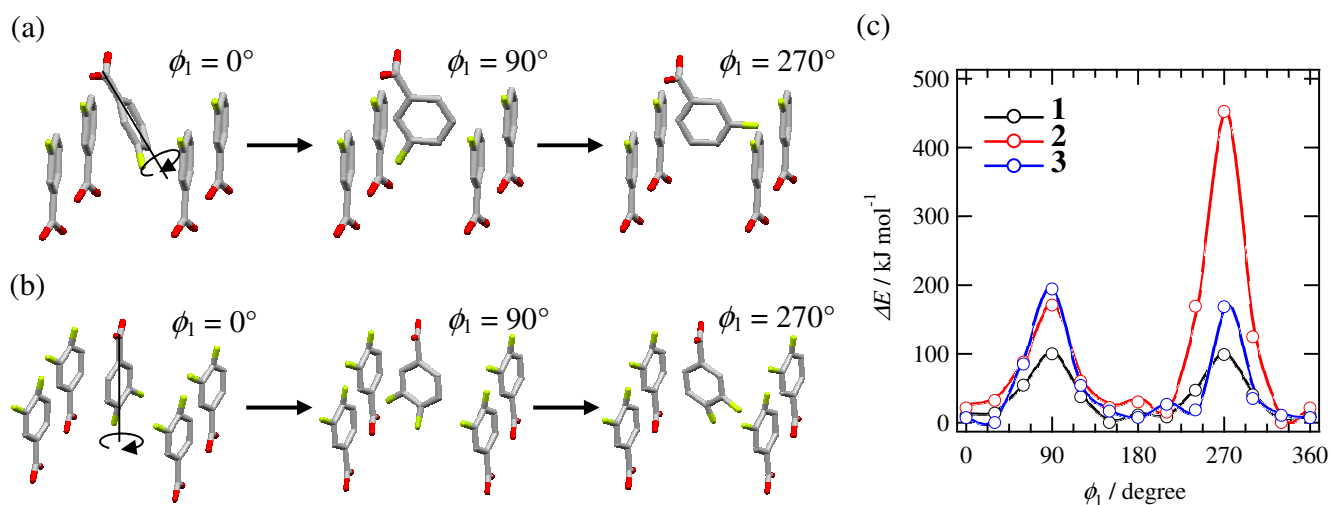


**Figure S7.** Potential energy curves for the molecular rotations of polar F<sub>x</sub>BA ligands in crystals **1**, **2**, and **3**. Model structures of (a) (3-FBA)<sub>5</sub> and (b) (2,3-F<sub>2</sub>BA)<sub>5</sub> assemblies in crystals **2** and **3**, where the rotation of central 3-FBA and 2,3-F<sub>2</sub>BA ligands were calculated in the fixed arrangement of the neighboring four ligands. (c) Relative energy  $\Delta E$  vs rotation angle  $\phi_1$  plots for the molecular rotations of three polar F<sub>x</sub>BA ligands in crystals **1**, **2** and **3** using a B3LYP/3-21G(d) basis set. Each line was a guide for eye.

To evaluate the possible molecular motions in each crystal, the DFT calculation was carried out based on a B3LYP/3-21G(d) basis set. One F<sub>x</sub>BA ligand was rotated every  $30^\circ$  with a rotation angle  $\phi_1$  along the C–COO<sup>−</sup> bond, which was surrounded by four neighboring independent F<sub>x</sub>BA ligands (Figures S7a and S7b). Although the cooperative molecular motions should be assumed in the crystalline state, the potential energy in the present theoretical calculations overestimated the magnitude of potential energy barrier. Figure S7 summarizes the potential energy curves for ligand rotation of 4-FBA, 3-FBA, and 3,4-F<sub>2</sub>BA. The double minimum type potential energy curve with two energy minima at  $\phi = 0$  and  $180^\circ$  were obtained in all crystals, where the potential energy barriers ( $\Delta E$ ) were appeared at  $\phi = 90$  and  $270^\circ$ . Although the arrangement of F<sub>x</sub>BA ligands in crystals **1** and **3** was parallel due to the dipole-dipole

interaction induced by fluorine atom at the *para*-position in benzoate, the  $\Delta E \sim 100 \text{ kJ mol}^{-1}$  at  $\phi = 90^\circ$  in crystal **1** was almost the half of that of  $\Delta E \sim 200 \text{ kJ mol}^{-1}$  in crystal **2** due to less steric repulsive effect for the rotations of *p*-FBA. On the contrary, asymmetrical potential energy curve at different  $\Delta E$ -maxima at  $\phi = 90$  and  $270^\circ$  was observed in the molecular rotation of crystal **2**, which completely suppressed the fully  $360^\circ$ -rotation from  $\phi = 0$  to  $360^\circ$ . The asymmetry was arose from the asymmetrical repulsion between the 3-FBA ligands (Figure S7a). The two-fold flip-flop rotation above 350 K has been reported in the  $\Delta E \sim 270 \text{ kJ mol}^{-1}$  of the ferroelectric supramolecular rotator in (*m*-FAni<sup>+</sup>)(DB[18]crown-6)[Ni(dmit)<sub>2</sub>]<sup>-</sup> crystal. From the magnitude of  $\Delta E$ , the two-fold flip-flop motion of polar 4-FBA ligands can be assumed in crystal **1**, whereas relatively large  $\Delta E > 200 \text{ kJ mol}^{-1}$  for crystal **3** should be difficult to rotate fully in the molecular assemblies. Therefore, the thermally activated dipole fluctuations of polar 3,4-F<sub>2</sub>BA ligands occurred around the structural phase transition temperatures of crystals **3**.